Avo Analysis By Simultaneous P-P And P-S Weighted Stacking Applied To 3C-3D Seismic Data

Muhammad Edisar, S.Si, M.T
Jurusan Fisika FMIPA Univ.Riau, Kampus Binawidya Pekanbaru : E-mail : edisar_m@yahoo.com

Abstract
A method has been developed to simultaneously invert P-P and P-S pre-stack seismic data to extract estimates of compressional and shear impedance values. This method uses separately processed P-P and P-S data volumes, each consisting of a series of migrated limited-offset data volumes. These offset data volumes for the P-P and P-S datasets are then weighted and summed to form two separate data volumes representing fractional compressional and shear impedance estimates. These data volumes can thus be used correlate anomalous compressional and shear impedance values that can be related to lithology and pore fluid content changes. This method is compared to a stand-alone P-wave weighted stacking method using a 3C-3D dataset. Initial results show the inclusion of the P-S data significantly improves both compressional and shear impedance estimates.

Keyword : Seismic, Shear Impedance, Anomalous compressional

Introduction

A number of authors have demonstrated the utility of combined AVO analyses using P-P, P-S and S-S modes (Garotta and Granger, 1987, Miles and Gassaway, 1989). In an effort to constrain some of the problems inherent with standard P-P weighted stacking methods, Stewart (1990) developed a joint P-P and P-S weighted stacking technique. This method while maintaining the robustness of the P-wave weighted stacking technique (Smith and Gidlow, 1987) has the benefit of data redundancy provided by the converted wave data. Since changes in RPP are partially controlled by the conversion of P-wave energy into S-wave energy, RPP has a partial dependence on the shear velocity. By contrast, converted wave (P-S) reflectivity is generally more dependant on S-wave velocities (Danbom and Domenico, 1986). This effect can easily be seen in the Aki and Richards (1980) Zoeppritz equation approximations.

Theory

The Zoeppritz equations fully describe the relationship between incident, reflected and transmitted P and S plane waves on either side of a plane interface. The Zoeppritz equation approximations of Aki and Richards (1980) simplify these equations into a form, linear in fractional elastic parameters, as follows:

$$R_{pp}(\theta)=\frac{1}{2}\left(1-4\frac{\beta^2}{\alpha^2}\sin^2\theta\right)\frac{\Delta\rho}{\rho}+\frac{1}{2\cos^2\theta}\frac{\Delta\alpha}{\alpha}-\frac{4\beta^2}{\alpha^2}\sin^2\frac{\Delta\beta}{\beta} \quad (1)$$

$$R_{ps}(\theta)=\frac{-\alpha\tan\varphi}{2\beta}\left[\left(1-\frac{2\beta^2}{\alpha^2}\sin^2\theta+\frac{2\beta}{\alpha}\cos\theta\cos\varphi\right)\frac{\Delta\rho}{\rho}-\left(\frac{4\beta^2}{\alpha^2}\sin^2\theta-\frac{4\beta}{\alpha}\cos\theta\cos\varphi\right)\frac{\Delta\beta}{\beta}\right] \quad (2)$$

where α, β, ρ are the average P-wave, S-wave and density values across an interface, $\Delta\alpha$, $\Delta\beta$, $\Delta\rho$ are the P-wave, S-wave and density contrasts across an interface, θ is the average of the P-wave angle of reflection and transmission across the interface, and φ is the average of the converted wave angle of reflection and transmission across the interface. Equations (1) and (2) are accurate for small relative changes in elastic parameters and small incidence angles (Aki and Richards, 1980).

These equations can be expressed as functions of density, compressional and shear impedance values:

$$R_{pp}(\theta)=\left(\frac{1+\tan^2\theta}{2}\right)\frac{\Delta I}{I}-4\frac{\beta^2}{\alpha^2}\sin^2\theta\frac{\Delta J}{J}-\left(\frac{1}{2}\tan^2\theta-2\frac{\beta^2}{\alpha^2}\sin^2\theta\right)\frac{\Delta\rho}{\rho} \quad (3)$$

$$R_{ps}(\theta,\varphi)=\frac{-\alpha\tan\varphi}{2\beta}\left[\left(1+\frac{2\beta^2}{\alpha^2}\sin^2\theta-\frac{2\beta}{\alpha}\cos\theta\cos\varphi\right)\frac{\Delta\rho}{\rho}-\left(\frac{4\beta^2}{\alpha^2}\sin^2\theta-\frac{4\beta}{\alpha}\cos\theta\cos\varphi\right)\frac{\Delta J}{J}\right] \quad (4)$$

where

$$\frac{\Delta I}{I}=\left(\frac{\Delta\alpha}{\alpha}+\frac{\Delta\rho}{\rho}\right) \qquad \frac{\Delta J}{J}=\left(\frac{\Delta\beta}{\beta}+\frac{\Delta\rho}{\rho}\right)$$

Following Smith and Gidlow (1987) we can further define a fractional VP/VS ratio or Pseudo-Poisson's ratio reflectivity as the difference between fractional compressional and shear impedance values.

$$\frac{\Delta\sigma}{\sigma}=\frac{\Delta I}{I}-\frac{\Delta J}{J}=\frac{\Delta\left(\alpha/\beta\right)}{\left(\alpha/\beta\right)} \quad (5)$$

It can be shown that the fractional density term in equation (3) is small for angles of incidence less than 35 degrees and β/α values between 1.5 and 2.0 (Gidlow et al., 1992). The fractional density term in equation (4) can be treated in one of two ways. First, it can be neglected which can be considered valid for small incidence angles and β/α values of 0.5, or for near-zero density?contrasts. Second, it can be written as:

$$\frac{\Delta\rho}{\rho}=\frac{1}{5}\left(4\frac{\Delta\rho}{\rho}+\frac{\Delta\rho}{\rho}\right)=\frac{1}{5}\left(\frac{\Delta\alpha}{\alpha}+\frac{\Delta\rho}{\rho}\right)=\frac{1}{5}\frac{\Delta I}{I} \quad (6)$$

by differentiating Gardner's relation (Gardner et al., 1974) which relates density and compressional velocity as $1/4(\Delta\alpha/\alpha) = \Delta\rho/\rho$. Thus equations (3) and (4) can be written as weighted linear functions in $\Delta I/I$ and $\Delta J/J$ as follows:

$$R_{PP}(\theta) = a(\theta)\frac{\Delta I}{I} + b(\theta)\frac{\Delta J}{J} \tag{7}$$

$$R_{PS}(\theta,\varphi) = c(\theta,\varphi)\frac{\Delta I}{I} + d(\theta,\varphi)\frac{\Delta J}{J} \tag{8}$$

Given estimates of RPP and RPS over a range of incidence angles, the least-squares inverse of equations (7) and (8) can thus be obtained (Stewart, 1990, Larsen et al., 1998) to give:

$$\frac{\Delta I}{I} = \sum_i \left[R_{PP} \frac{a_i \sum_j (b_j^2 + d_j^2) - b_i \sum_j (a_j b_j + c_j d_j)}{\sum_j (a_j^2 + c_j^2) \sum_j (b_j^2 + d_j^2) - \left[\sum_j (a_j b_j + c_j d_j)\right]^2} + R_{PS} \frac{c_i \sum_j (b_j^2 + d_j^2) - d_i \sum_j (a_j b_j + c_j d_j)}{\sum_j (a_j^2 + c_j^2) \sum_j (b_j^2 + d_j^2) - \left[\sum_j (a_j b_j + c_j d_j)\right]^2} \right] \tag{9}$$

$$\frac{\Delta J}{J} = \sum_i \left[R_{PP} \frac{b_i \sum_j (a_j^2 + c_j^2) - a_i \sum_j (a_j b_j + c_j d_j)}{\sum_j (a_j^2 + c_j^2) \sum_j (b_j^2 + d_j^2) - \left[\sum_j (a_j b_j + c_j d_j)\right]^2} + R_{PS} \frac{d_i \sum_j (a_j^2 + c_j^2) - c_i \sum_j (a_j b_j + c_j d_j)}{\sum_j (a_j^2 + c_j^2) \sum_j (b_j^2 + d_j^2) - \left[\sum_j (a_j b_j + c_j d_j)\right]^2} \right] \tag{10}$$

Where the summation is over all incidence angles (or source-receiver offsets), RPP and RPS represent suitably processed and correlated P-P and P-S seismic data, and a, b, c and d are offset-dependant model-based weights. Notice the similarity of these equations to stand-alone P-wave methods (Smith and Gidlow, 1987; Gidlow et al., 1992; Fatti et al., 1994).

Examples

This inversion method was tested with data from the Mory field 3C-3D survey (Margrave et al., 1998). The target of most interest in this study is the gas-filled, lower Cretaceous age, upper-Glauconitic, channel interval. Previous P-P AVO studies at Mory filed have shown a significant P-wave reflectivity anomaly associated with the upper channel (Simin et al., 1996; Dufour et al., 1998). Data was first flattened relative to an easily identifiable regional seismic horizon just above the channel zone. Following established data processing techniques (Lu and Margrave, 1998), the P-P and P-S data were formed into 5 limited-offset migrated data volumes. Each limited-offset data volume covers an offset range at the zone of interest (Glauconitic channel). For the purposes of this study, a single pass 3D phase-shift migration was used following stacking of each offset range. The final P-P and P-S offset volumes were trace-equalized prior to output. To restore the average expected AVO behavior, an elastic-wave multioffset synthetic seismogram was created from dipole sonic information. The limited offset data volumes were then scaled to have the same average RMS amplitudes as the synthetic. Next, the offset dependant weights (a, b, c and d in equations 5 and 6) were calculated using a highly smoothed velocity-depth model derived from well 09-08. Finally, 3D volumes representing estimates of $\Delta I/I$ and $\Delta J/J$ were formed using equations (7) and (8). Results from well log analysis indicates a strong negative compressional impedance ($\Delta I/I$) anomaly, and a relatively weak, positive shear impedance ($\Delta J/J$) anomaly in the channel zone. Table 1 summarizes the expected estimates of $\Delta I/I$, $\Delta J/J$ and $\Delta\sigma/\sigma$ at the stratigraphic level of figure 1 from blocked wells logs in the area of study and compares these values to those obtained from the inversions.

Both P-P and simultaneous P-P and P-S methods predict the general trend of the Glauconitic sand channel. The P-P method does not adequately predict the extent of the P-wave impedance anomaly between wells 01-08 and 16-08. The shear impedance estimates are generally smaller in magnitude for the simultaneous inversion method, which more closely corresponds to the observed values in table 1. There is however little shear velocity control in the channel trend between wells 01-08 and 16-08.

Conclusions

A simultaneous P-P and P-S weighted stacking inversion method has been implemented and compared to another standard method utilizing only P-P seismic data. Initial results show there is a general improvement using both types of data, events appear more coherent and signal-to-noise appears to have increased.

Table 1: Expected values of $\Delta I/I$, $\Delta J/J$ and $\Delta\sigma/\sigma$ from blocked sonic logs at the Upper Glauconitic channel interface. Values of $\Delta J/J$ and $\Delta\sigma/\sigma$ are derived from full-waveform sonic logs and compared with values from the maps in figure 1.

Well	01-08[1]	08-08[1]	09-08[1]	16-08[1]	12-16[2]	13-16[3]	09-17[3]	
$\Delta I/I$	-0.129	-0.141	-0.209	-0.173	-0.110	-0.175	-0.057	calculated results from well logs
$\Delta J/J$	---	0.015	---	---	-0.050	---	-0.037	
$\Delta\sigma/\sigma$	---	-0.156	---	---	0.039	---	-0.020	
$\Delta I/I$	-0.012	-0.140	-0.210	-0.124	-0.130	-0.183	-0.089	P-P inversion method
$\Delta J/J$	-0.026	0.052	0.053	0.053	-0.048	-0.014	-0.034	
$\Delta\sigma/\sigma$	0.014	-0.192	-0.263	-0.177	0.035	-0.169	-0.055	
$\Delta I/I$	-0.113	-0.138	-0.218	-0.176	-0.120	-0.177	-0.058	Simultaneous P-P and P-S inversion method
$\Delta J/J$	-0.021	0.012	0.017	0.013	-0.051	-0.041	-0.040	
$\Delta\sigma/\sigma$	-0.092	-0.150	-0.235	-0.189	0.039	-0.136	-0.018	

Sand channel well, 2 Shale plugged channel well, 3 Regional well

References

Aki, K., and Richards, P.G., 1980, Quantitative seismology: Theory and methods, Vol. 1: W.H. Freeman and Co.

Danbom, S.H., and Domenico, S.N., 1986, Shear-wave exploration: Geophysical Development Series, Volume 1, Soc. Expl. Geophys.

Dufuor, J., Squires, J., Edmunds, A. and Shook, I., 1998, Integrated geological and geophysical interpretation of the Blackfoot area, Southern Alberta: Geo-Triad Expanded Abstracts, 234-236.

Fatti, J.L., Smith, G.C., Vail, P.J., Strauss, P.J. and Levitt, P.R., 1994, Detection of gas in sandstone reservoirs using AVO analysis: A 3-D seismic case history using the Geostack technique: Geophysics, 59, 1362-1376.

Gardner, G.H.F., Gardner, L.W., and Gregory, A.R., 1974, Formation velocity and density, the diagnostic basics for stratigraphic traps: Geophysics, 39, 770-780.

Garotta, R., and Granger, P.Y., 1987, Comparison of responses of compressional and converted waves on a gas sand: 57th Ann.Internat. Mtg., Soc. Expl. Geophys., Expanded Abstracts, 627-630.

Gidlow, P.M., Smith, G.C., Vail, P.J., 1992, Hydrocarbon detection using fluid factor traces; A case history: SEG/EAGE Workshop.

Larsen, J.A., Margrave, G.F., Lu, H., and Potter, C.C., Simulta-

neous P-P and P-S inversion by weighted stacking applied to the Blackfoot 3C-3D: The CREWES Research Report, Vol. 10, Ch. 50.

Lu, H., and Margrave, G.F., 1998, Reprocessing of the Blackfoot 3C-3D dataset: The CREWES Research Report, Vol. 10, Ch. 31.

Margrave, G.F., Lawton, D.C., and Stewart, R.R., Interpreting channel sands with 3C-3D seismic data: The Leading Edge, 1998,509-513.

Miles, D.R., and Gassaway, G.S., 1989, Three-component AVO analysis: 59th Ann. Internat. Mtg., Soc. Expl. Geophys., Expanded Abstracts, 706-708.

Simin, V., Margrave, G.F. and Yang, G.C., 1996, AVO measurements for P-P and P-S data in the Blackfoot 3C-3D dataset: The CREWES Research Report, Vol. 8, ch. 42.

Smith, G.C., and Gidlow, P.M., 1987, Weighted stacking for rock property estimation and detection of gas: Geophysical Prospecting 35, 993-1014.

Stewart, R.R., 1990, Joint P and P-SV Inversion: The CREWES Research Report, Vol. 3, 112-115

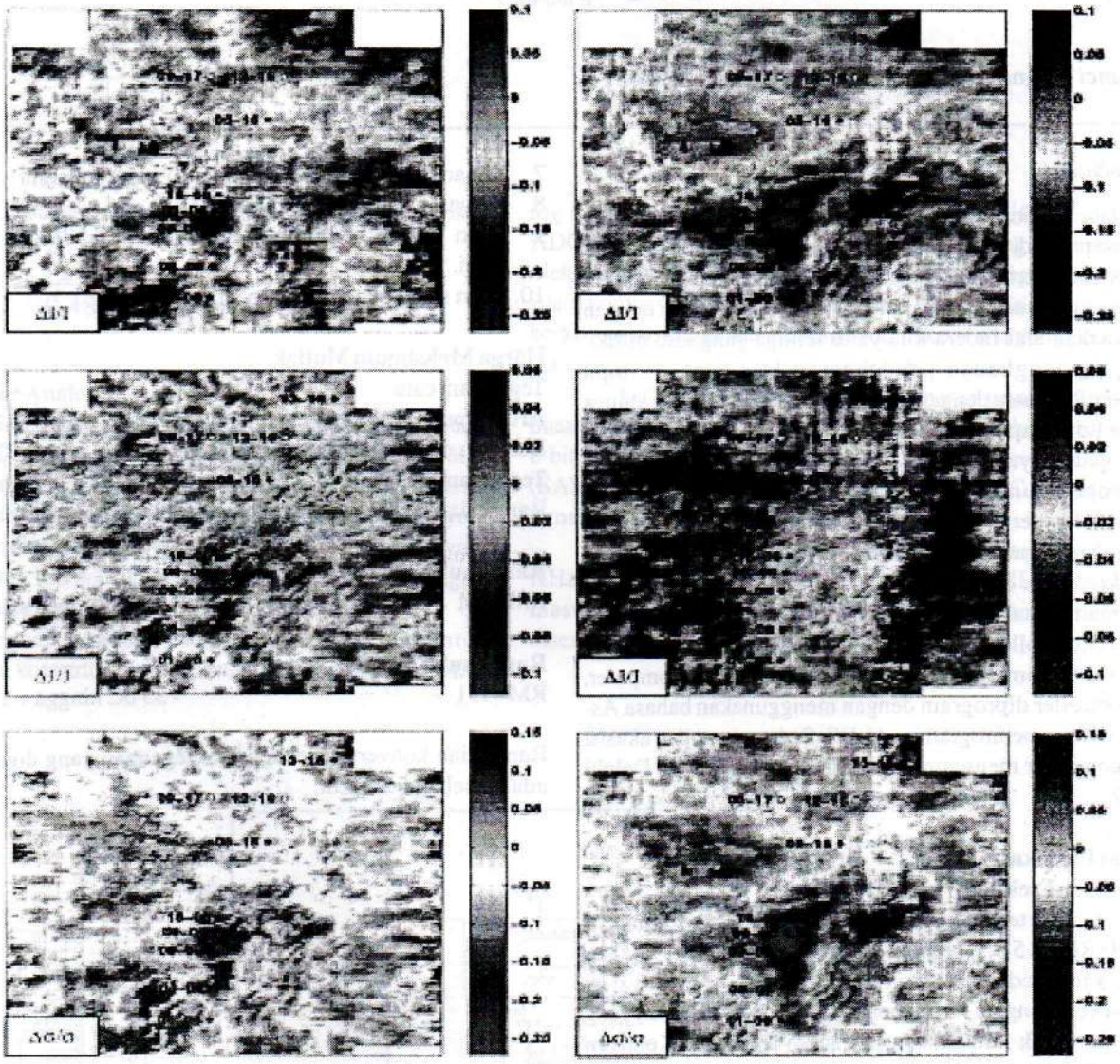

Figure 1: Areal views at the top of the upper Glauconitic channel gas zone. Fractional P-wave impedance estimates for P-P (upper left) and both P-P and P-S data (upper right). Fractional shear impedance estimates for P-P (middle left) and both P-P and P-S (middle right). Pseudo-Poisson's ratio (fractional Vp/Vs ratio) estimates for P-P (lower left) and both P-P and P-S (lower left). Note the general improvement in signal-to-noise using both P-P and P-S seismic data. Black dots indicate producing oil wells along the channel trend. White dots indicate shale plugged or regional wells. The main channel body is oriented roughly north-south and extends from 01-08 to 16-08. The upper channel thins between wells 16-08 and 13-16, with well 12-16 representing a shale plugged channel body.